

DYNAMIC RESPONSE OF A HEAT CONDUCTING SOLID BAR OF POLYGONAL CROSS SECTIONS SUBJECTED TO MOVING HEAT SOURCE

R. Selvamani

Department of Mathematics Karunya University, Coimbatore, TamilNadu, India.

e-mail: selvam1729@gmail.com

Abstract. The dynamic response of a heat conducting solid bar of polygonal cross section subjected to moving heat source is discussed using the Fourier expansion collocation method (FECM). The equations of motion are formulated using the three dimensional constitutive equation of elasticity and generalized thermo elastic equation composed of linear homogeneous isotropic material. Three displacement potential functions are introduced to uncouple the equations of motion and the heat conduction. The frequency equations are obtained by satisfying the boundary conditions along the surface of the polygonal solid bar using Fourier expansion collocation method. The numerical calculations are carried out for triangular, square, pentagonal and hexagonal cross sectional bars with different moving heat source speeds. Dispersion curves are plotted for longitudinal and flexural (antisymmetric) modes of non dimensional frequency.

1. Introduction

The study of dynamic response of heat conducting solid bar is significant in the ultrasonic inspection of materials, vibration of engineering structures, atomic physics, industrial engineering, thermal power plants, submarine structures, pressure vessel, aerospace, chemical pipes and metallurgical process. The theory of moving sources of heat has been instrumental in providing the welding engineer with a scientific criterion for the weld ability of steel and surface hardening of metallic alloys. The importance of thermal stresses in causing structural damages and changes in functioning of the structure is well recognized whenever thermal stress environments are involved. Therefore, the ability to predict thermodynamics stresses induced by moving heat sources in structures with polygonal cross sections are essential for the proper and safe design and the knowledge of its response during the service in these severe thermal environments. The dispersion of displacement, temperature change and perturbed magnetic field in case of fundamental modes for the symmetric and antisymmetric cases of the cylindrical panel is playing a vital role in smart material applications. This type of model analysis is very important in bio sensing applications in nuclear magnetic resonance (NMR), magnetic resonance imaging (MRI) and echo planar imaging (EPI).

Gazis [1] has studied the most general form of harmonic waves in hollow cylinder of circular cross section of infinite length. He presented in detail the frequency equation in Part I and numerical results in Part II. Mirsky [2] analyzed the wave propagation in transversely isotropic circular cylinders of infinite length and presented the frequency equation in Part I and numerical results in Part II. Nagaya [3-6] discussed wave propagation in an infinite bar of arbitrary cross section and the wave propagation in an infinite cylinder of both inner and outer

The problems involving a moving heat source plays vital role in thermal fields due to its extensive engineering applications, such as continuous annealing after cold working, pulsed-laser cutting and welding, and high speed machining and grinding etc. Al-Huniti et al. [27] studied the dynamic responses of a copper rod due to a moving heat source under the wave type heat conduction model and by means of the Laplace transform the temperature was obtained directly from the heat conduction equation. Baksi et al. [28] considered a three-dimensional problem for a homogeneous, orthotropic, electrically as well as thermally conducting infinite rotating elastic medium with heat source by the eigen value approach. Lykotrafitis and Georgiadis [29] studied the three-dimensional steady-state thermo_elastodynamic problem of moving sources over a half space. Hsieh [30] presented the exact solution of Stefan problems related to a moving line heat source in a quasi-stationary state.

In this paper, the free vibration of a generalized thermoelastic solid cylinder of polygonal (triangular, square, pentagonal and hexagonal) cross section is studied using the Fourier expansion collocation method based on Sububi's generalized theory [31]. The computed nondimensional wave numbers are plotted as graphs.

2. Governing equations

The generalized theories of thermoelasticity are the constitutive equations in which the functions are temperature rate dependent. The constitutive equations for a linear isotropic thermoelastic medium, the stresses σ_{ij} , expressed in cylindrical coordinates, are

$$\sigma_{rr} = \lambda(e_{rr} + e_{\theta\theta} + e_{zz}) + 2\mu e_{rr} - \beta(T + \eta T_{,t}), \quad (1a)$$

$$\sigma_{\theta\theta} = \lambda(e_{rr} + e_{\theta\theta} + e_{zz}) + 2\mu e_{\theta\theta} - \beta(T + \eta T_{,t}), \quad (1b)$$

$$\sigma_{zz} = \lambda(e_{rr} + e_{\theta\theta} + e_{zz}) + 2\mu e_{zz} - \beta(T + \eta T_{,t}), \quad (1c)$$

$$\sigma_{r\theta} = 2\mu\gamma_{r\theta}, \quad \sigma_{\theta z} = 2\mu\gamma_{\theta z}, \quad \sigma_{rz} = 2\mu\gamma_{rz}. \quad (1d,e,f)$$

where e_{ij} are the strain components, β is the thermal stress coefficients, T is the temperature, η is of generalized thermo elasticity, t is the time, λ and μ are Lamé' constants. The strain e_{ij} are related to the displacements are given by

$$e_{rr} = u_{,r}, \quad e_{\theta\theta} = r^{-1}(u + v_{,\theta}), \quad e_{zz} = w_{,z}, \quad (2a)$$

$$\gamma_{r\theta} = v_{,r} - r^{-1}(v - u_{,\theta}), \quad \gamma_{z\theta} = v_{,z} + r^{-1}w_{,\theta}, \quad \gamma_{rz} = w_{,r} + u_{,z}, \quad (2b)$$

in which u , v and w are the displacement components along radial, circumferential and axial directions respectively. The comma in the subscripts denotes the partial differentiation with respect to the variables.

3. Equations of motion

The three dimensional equations of motion and the heat conduction equation in the reference system r , θ and z are

$$\sigma_{r,r} + r^{-1}\sigma_{r\theta,\theta} + \sigma_{rz,z} + r^{-1}(\sigma_{rr} - \sigma_{\theta\theta}) = \rho u_{,tt}, \quad (3a)$$

$$\sigma_{r\theta,r} + r^{-1}\sigma_{\theta\theta,\theta} + \sigma_{,rz} + \sigma_{\theta z,z} + 2r^{-1}\sigma_{r\theta} = \rho v_{,tt}, \quad (3b)$$

$$T(r, \theta, z, t) = ((\lambda + 2\mu)/\beta a^2) \sum_{n=0}^{\infty} [T_n + \bar{T}_n] e^{i(kz + \omega t)}, \quad (6d)$$

where $\varepsilon_n = \frac{1}{2}$ for $n=0$, $\varepsilon_n = 1$ for $n \geq 1$, $i = \sqrt{-1}$, k is the wave number, ω is the frequency, $\phi_n(r, \theta)$, $W_n(r, \theta)$, $T_n(r, \theta)$, $\psi_n(r, \theta)$, $\bar{\phi}_n(r, \theta)$, $\bar{W}_n(r, \theta)$, $\bar{T}_n(r, \theta)$, $\bar{\psi}_n(r, \theta)$ are the displacement potentials and a is the geometrical parameter of the cylinder.

Introducing the irrotational velocity $c_1^2 = (\lambda + 2\mu)/\rho$ and dimensionless quantities such as $\varsigma = ka$, $\bar{z} = z/a$, $T_a = t\sqrt{\mu/\rho}/a$, $x = r/a$, $\alpha' = c_1 a/\kappa$, $\Omega^2 = \omega^2 a^2/c_1^2$, $\chi_1 = \frac{T_0 a}{\rho^2 c_v c_1 \kappa} \beta^2$,

$Q^* = \frac{Q_0 v}{i \chi_1 \Omega}$, $\chi_2 = \frac{c_1^2}{c_v \kappa} \tau$, $\chi_3 = \frac{c_1}{a} \eta$, and $\chi_4 = 1/(2 + \bar{\lambda})$, and using Eqs. (5) and (6) in Eqs. (4), we obtain

$$(\nabla^2 + \Omega^2 - \chi_4 \varsigma^2) \phi_n - \varsigma(1 + \bar{\lambda}) \chi_4 W_n - (1 + i \chi_3 \Omega) T_n = 0, \quad (7a)$$

$$\varsigma(1 + \bar{\lambda}) \chi_4 \nabla^2 \phi_n + (\chi_4 \nabla^2 + \Omega^2 - \varsigma^2) W_n - \varsigma(1 + i \chi_3 \Omega) T_n = 0, \quad (7b)$$

$$-i \chi_1 \Omega \nabla^2 \phi_n + i \chi_1 \varsigma \Omega W_n + (\nabla^2 - i \alpha' \Omega + \chi_2 - Q^*) T_n = 0, \quad (7c)$$

$$(\nabla^2 + (2 + \bar{\lambda}) \Omega^2 - \varsigma^2) \psi_n = 0, \quad (7d)$$

where $\nabla^2 \equiv \partial^2/\partial x^2 + x^{-1} \partial/\partial x + x^{-2} \partial^2/\partial \theta^2$.

The parameters defined in Eqs. (7), namely, χ_1 couples the equations corresponding to the elastic wave propagation and the heat conduction which is called the coupling factor; the coefficient χ_2 , which is introduced by the theory of generalized thermoelasticity, may render the governing system of equations hyperbolic. The parameter χ_3 is the coefficient of the term indicating the difference between empirical and thermodynamic temperatures.

Rewriting Eqs. (7) results in the following vanishing determinant form

$$\begin{vmatrix} (\nabla^2 + \Omega^2 - \chi_4 \varsigma^2) & -\varsigma \chi_4 (1 + \bar{\lambda}) & (1 + i \chi_3 \Omega) \\ \varsigma \chi_4 (1 + \bar{\lambda}) & (\nabla^2 \chi_4 + \Omega^2 - \varsigma^2) & -\varsigma(1 + i \chi_3 \Omega) \\ -i \chi_1 \Omega & i \varsigma \chi_1 \Omega & (\nabla^2 - i \alpha' \Omega + \chi_2 - Q^*) \end{vmatrix} (\phi_n, W_n, T_n) = 0. \quad (8)$$

Equation (8), on simplification reduces to the following differential equation

$$(A \nabla^6 + B \nabla^4 + C \nabla^2 + D)(\phi_n, W_n, T_n) = 0, \quad (9)$$

where

$$A = \chi_4, \quad (10a)$$

$$B = \chi_4 (\Omega^2 - \chi_4 \varsigma^2 + \chi_2 - i \alpha' \Omega) + \varsigma^2 \chi_4^2 (1 + \bar{\lambda})^2 + (\Omega^2 - \varsigma^2), \quad (10b)$$

$$C = i \varsigma \Omega (1 + i \chi_3 \Omega) (\varsigma^2 + \varsigma^2 \chi_4 (1 + \bar{\lambda}) + \chi_4)$$

where $(\alpha_4 a)^2 = \Omega^2 - \zeta^2$. If $(\alpha_j a)^2 < 0$, ($j=1,2,3$), then the Bessel function J_n is to be replaced by the modified Bessel function I_n .

In this problem, the free vibration of a generalized thermoelastic solid bar of polygonal cross section is considered. Since the boundary is irregular, the Fourier expansion collocation method is applied on the boundary of the cross section. Thus, the boundary conditions obtained are

$$\left(\sigma_{pp}\right)_l = \left(\sigma_{pq}\right)_l = \left(\sigma_{zp}\right)_l = (T)_l = 0. \quad (17)$$

where p is the coordinate normal to the boundary and q is the coordinate in the tangential direction. Here σ_{pp} is the normal stress, σ_{pq} and σ_{zp} are the shearing stresses and $()_l$ is the value at the l -th segment of the boundary. Since the coordinate p and q are functions of r and θ , it is difficult to find transformed expressions for the stresses. Therefore the curved boundary is divided into small segments such that the variations of the stresses are assumed to be constant. Assuming the angle γ_l , between the normal to the segment and the reference axis to be constant, the transformed expressions for the stresses are followed by Nagaya [3-6]

$$\begin{aligned} \sigma_{pp} = 2\mu \left[u_{,r} \cos^2(\theta - \gamma_l) + r^{-1}(u + v_{,\theta}) \sin^2(\theta - \gamma_l) + 0.5(r^{-1}[u - u_{,\theta}] - v_{,r}) \sin 2(\theta - \gamma_l) \right] \\ + \lambda (u_{,r} + r^{-1}(u + v_{,\theta}) + w_{,z}), \end{aligned} \quad (18a)$$

$$\sigma_{pq} = \mu \left[(u_{,r} - r^{-1}(v_{,\theta} + u)) \sin 2(\theta - \gamma_l) + (r^{-1}(u_{,\theta} - v) + v_{,r}) \cos 2(\theta - \gamma_l) \right], \quad (18b)$$

$$\sigma_{zq} = \mu \left[(u_{,z} + w_{,r}) \cos(\theta - \gamma_l) - (v_{,z} + r^{-1}w_{,\theta}) \sin(\theta - \gamma_l) \right]. \quad (18c)$$

Applying the Fourier expansion collocation method along the curved surface of the boundary, the transformed expressions for the stresses are

$$\left[(S_{pp})_l + (\bar{S}_{pp})_l \right] e^{i(\zeta \bar{z} + \Omega T_a)} = 0, \quad \left[(S_{pq})_l + (\bar{S}_{pq})_l \right] e^{i(\zeta \bar{z} + \Omega T_a)} = 0, \quad (19a,b)$$

$$\left[(S_{zp})_l + (\bar{S}_{zp})_l \right] e^{i(\zeta \bar{z} + \Omega T_a)} = 0, \quad \left[(S_t)_l + (\bar{S}_t)_l \right] e^{i(\zeta \bar{z} + \Omega T_a)} = 0, \quad (19c,d)$$

where,

$$S_{pp} = 0.5(A_{10}e_0^1 + A_{20}e_0^2 + A_{30}e_0^3 + B_{50}e_0^5) + \sum_{n=1}^{\infty} (A_{1n}e_n^1 + A_{2n}e_n^2 + A_{3n}e_n^3 + A_{4n}e_n^4 + B_{5n}e_n^5), \quad (20a)$$

$$S_{pq} = 0.5(A_{10}f_0^1 + A_{20}f_0^2 + A_{30}f_0^3) + \sum_{n=1}^{\infty} (A_{1n}f_n^1 + A_{2n}f_n^2 + A_{3n}f_n^3 + A_{4n}f_n^4), \quad (20b)$$

$$S_{zp} = 0.5(A_{10}g_0^1 + A_{20}g_0^2 + A_{30}g_0^3) + \sum_{n=1}^{\infty} (A_{1n}f_n^1 + A_{2n}f_n^2 + A_{3n}f_n^3 + A_{4n}f_n^4), \quad (20c)$$

$$S_t = 0.5(A_{10}k_0^1 + A_{20}k_0^2 + A_{30}k_0^3) + \sum_{n=1}^{\infty} (A_{1n}k_n^1 + A_{2n}k_n^2 + A_{3n}k_n^3), \quad (20d)$$

$$\bar{S}_{pp} = 0.5\bar{A}_{40}\bar{e}_0^{-4} + \sum_{n=1}^{\infty} \left(\bar{A}_{1n}\bar{e}_n^{-1} + \bar{A}_{2n}\bar{e}_n^{-2} + \bar{A}_{3n}\bar{e}_n^{-3} + \bar{A}_{4n}\bar{e}_n^{-4} + \bar{B}_{5n}\bar{e}_n^{-5} \right), \quad (21a)$$

where,

$$E_{mn}^j = (2\varepsilon_n/\pi) \sum_{l=1}^L \int_{\theta_{l-1}}^{\theta_l} e_n^j(R_l, \theta) \cos m\theta d\theta, \quad (24a)$$

$$F_{mn}^j = (2\varepsilon_n/\pi) \sum_{l=1}^L \int_{\theta_{l-1}}^{\theta_l} f_n^j(R_l, \theta) \sin m\theta d\theta, \quad (24b)$$

$$G_{mn}^j = (2\varepsilon_n/\pi) \sum_{l=1}^L \int_{\theta_{l-1}}^{\theta_l} g_n^j(R_l, \theta) \cos m\theta d\theta, \quad (24c)$$

$$K_{mn}^j = (2\varepsilon_n/\pi) \sum_{l=1}^L \int_{\theta_{l-1}}^{\theta_l} k_n^j(R_l, \theta) \cos m\theta d\theta. \quad (24d)$$

Here $j=1,2,3,4$ and 5 , L is the number of segments, R_l is the coordinate r at the boundary and N is the number of terms in the Fourier series.

The boundary conditions for the antisymmetric mode are written in the form of a matrix as given below:

$$\begin{bmatrix} \bar{E}_{10}^4 & \bar{E}_{11}^1 & \cdots & \bar{E}_{1N}^1 & \bar{E}_{11}^2 & \cdots & \bar{E}_{1N}^2 & \bar{E}_{11}^3 & \cdots & \bar{E}_{1N}^3 & \bar{E}_{11}^4 & \cdots & \bar{E}_{1N}^4 & \bar{A}_{40} \\ \vdots & \vdots & & \vdots & \vdots & & \vdots & \vdots & & \vdots & \vdots & & \vdots & \bar{A}_{11} \\ \bar{E}_{N0}^4 & \bar{E}_{N1}^1 & \cdots & \bar{E}_{NN}^1 & \bar{E}_{N1}^2 & \cdots & \bar{E}_{NN}^2 & \bar{E}_{N1}^3 & \cdots & \bar{E}_{NN}^3 & \bar{E}_{N1}^4 & \cdots & \bar{E}_{NN}^4 & \vdots \\ \bar{F}_{00}^3 & \bar{F}_{01}^1 & \cdots & \bar{F}_{0N}^1 & \bar{F}_{01}^2 & \cdots & \bar{F}_{0N}^2 & \bar{F}_{01}^3 & \cdots & \bar{F}_{0N}^3 & \bar{F}_{01}^4 & \cdots & \bar{F}_{0N}^4 & \bar{A}_{1N} \\ \vdots & \vdots & & \vdots & \vdots & & \vdots & \vdots & & \vdots & \vdots & & \vdots & \vdots \\ \bar{F}_{N0}^4 & \bar{F}_{N1}^1 & \cdots & \bar{F}_{NN}^1 & \bar{F}_{N1}^2 & \cdots & \bar{F}_{NN}^2 & \bar{F}_{N1}^3 & \cdots & \bar{F}_{NN}^3 & \bar{F}_{N1}^4 & \cdots & \bar{F}_{NN}^4 & \vdots \\ \bar{G}_{10}^4 & \bar{G}_{11}^1 & \cdots & \bar{G}_{1N}^1 & \bar{G}_{11}^2 & \cdots & \bar{G}_{1N}^2 & \bar{G}_{11}^3 & \cdots & \bar{G}_{1N}^3 & \bar{G}_{11}^4 & \cdots & \bar{G}_{1N}^4 & \vdots \\ \vdots & \vdots & & \vdots & \vdots & & \vdots & \vdots & & \vdots & \vdots & & \vdots & \vdots \\ \bar{G}_{N0}^4 & \bar{G}_{N1}^1 & \cdots & \bar{G}_{NN}^1 & \bar{G}_{N1}^2 & \cdots & \bar{G}_{NN}^2 & \bar{G}_{N1}^3 & \cdots & \bar{G}_{NN}^3 & \bar{G}_{N1}^4 & \cdots & \bar{G}_{NN}^4 & \vdots \\ \bar{K}_{10}^4 & \bar{K}_{11}^1 & \cdots & \bar{K}_{1N}^1 & \bar{K}_{11}^2 & \cdots & \bar{K}_{1N}^2 & \bar{K}_{11}^3 & \cdots & \bar{K}_{1N}^3 & 0 & \cdots & 0 & \bar{A}_{41} \\ \vdots & \vdots & & \vdots & \vdots & & \vdots & \vdots & & \vdots & \vdots & & \vdots & \vdots \\ \bar{K}_{N0}^4 & \bar{K}_{N1}^1 & \cdots & \bar{K}_{NN}^1 & \bar{K}_{N1}^2 & \cdots & \bar{K}_{NN}^2 & \bar{K}_{N1}^3 & \cdots & \bar{K}_{NN}^3 & 0 & \cdots & 0 & \bar{A}_{4N} \end{bmatrix} = 0, \quad (25)$$

where,

$$\bar{E}_{mn}^j = (2\varepsilon_n/\pi) \sum_{l=1}^L \int_{\theta_{l-1}}^{\theta_l} \bar{e}_n^j(R_l, \theta) \sin m\theta d\theta, \quad \bar{F}_{mn}^j = (2\varepsilon_n/\pi) \sum_{l=1}^L \int_{\theta_{l-1}}^{\theta_l} \bar{f}_n^j(R_l, \theta) \cos m\theta d\theta, \quad (26a,b)$$

$$\bar{G}_{mn}^j = (2\varepsilon_n/\pi) \sum_{l=1}^L \int_{\theta_{l-1}}^{\theta_l} \bar{g}_n^j(R_l, \theta) \sin m\theta d\theta, \quad \bar{K}_{mn}^j = (2\varepsilon_n/\pi) \sum_{l=1}^L \int_{\theta_{l-1}}^{\theta_l} \bar{k}_n^j(R_l, \theta) \sin m\theta d\theta. \quad (26c,d)$$

5. Numerical results and discussion

In accordance with the theoretical results obtained in the previous sections and comparing these results with the literature results, some numerical analysis of the dispersion equation is carried out for triangular, square, pentagonal and hexagonal cross sectional bars. The secant method given by Antia (2002) is used to obtain the roots of the frequency equation. The material properties of copper at temperature 4.2 K are taken approximately as Poisson ratio $\nu=0.3$, the Young's modulus $E=2.139 \times 10^{11}\text{ N/m}^2$, $\lambda=8.20 \times 10^{11}\text{ kg/ms}^2$, $\mu=4.20 \times 10^{10}\text{ kg/ms}^2$, $c_v=9.1 \times 10^{-2}\text{ m}^2/\text{ks}^2$, $K=113 \times 10^2\text{ kg m/ks}^2$, $\rho=8.96 \times 10^3\text{ kg/m}^3$

Table 2. Comparison between the real $R(\xi)$ and imaginary $I(\xi)$ parts of frequency for longitudinal modes of the Square and Hexagonal cross-sectional bar with moving heat source velocities $\nu = 1$, $\nu = 2$ and $\nu = 3$.

Mode	Square						Hexagon					
	$\nu = 1$		$\nu = 2$		$\nu = 3$		$\nu = 1$		$\nu = 2$		$\nu = 3$	
	$R(\xi)$	$I(\xi)$	$R(\xi)$	$I(\xi)$	$R(\xi)$	$I(\xi)$	$R(\xi)$	$I(\xi)$	$R(\xi)$	$I(\xi)$	$R(\xi)$	$I(\xi)$
1	0.0914	0.0914	0.0904	0.0903	0.0842	0.0880	0.0942	0.0825	0.1002	0.0998	0.0957	0.1030
2	0.2717	0.2705	0.2732	0.2697	0.2619	0.2621	0.2766	0.2811	0.2984	0.3017	0.3717	0.2856
3	0.4594	0.4551	0.4611	0.4491	0.4397	0.4351	0.4622	0.4545	0.4993	0.5002	0.5014	0.5016
4	0.6466	0.6349	0.6526	0.6308	0.6209	0.6093	0.6530	0.6361	0.7081	0.7010	0.7084	0.7223
5	0.9564	0.9315	0.9429	0.8937	0.8971	0.8758	0.9168	0.8881	1.0098	0.9804	1.0076	

Table 3. Comparison between the real $R(\xi)$ and imaginary $I(\xi)$ parts of frequency for flexural antisymmetric modes of the Triangle and Pentagonal cross-sectional bar with moving heat source velocities $\nu = 1$, $\nu = 2$ and $\nu = 3$.

Mode	Triangle						Pentagon					
	$\nu = 1$		$\nu = 2$		$\nu = 3$		$\nu = 1$		$\nu = 2$		$\nu = 3$	
	$R(\xi)$	$I(\xi)$	$R(\xi)$	$I(\xi)$	$R(\xi)$	$I(\xi)$	$R(\xi)$	$I(\xi)$	$R(\xi)$	$I(\xi)$	$R(\xi)$	$I(\xi)$
1	0.0974	0.0870	0.0892	0.0889	0.0748	0.0753	0.0891	0.0889	0.0891	0.0889	0.0625	0.0646
2	0.2665	0.1596	0.2726	0.2677	0.2242	0.2353	0.2690	0.2655	0.2651	0.2591	0.1820	0.2254
3	0.4529	0.4357	0.4592	0.4488	0.4916	0.4023	0.4545	0.4401	0.4527	0.4296	0.3467	0.4148
4	0.7434	0.6147	0.6486	0.6316	0.5722	0.5590	0.6477	0.6170	0.6512	0.6220	0.5294	0.5783
5	0.9430	0.9012	0.9995	0.9409	0.8600	0.7878	0.9432	0.8914	0.9466	0.9003	0.7998	

Table 4. Comparison between the real $R(\xi)$ and imaginary $I(\xi)$ parts of frequency for flexural antisymmetric modes of the Square and Hexagonal cross-sectional bar moving heat source velocities $\nu = 1$, $\nu = 2$ and $\nu = 3$.

Mode	Square						Hexagon					
	$\nu = 1$		$\nu = 2$		$\nu = 3$		$\nu = 1$		$\nu = 2$		$\nu = 3$	
	$R(\xi)$	$I(\xi)$	$R(\xi)$	$I(\xi)$	$R(\xi)$	$I(\xi)$	$R(\xi)$	$I(\xi)$	$R(\xi)$	$I(\xi)$	$R(\xi)$	$I(\xi)$
1	0.1001	0.1001	0.0561	0.0345	0.0999	0.0999	0.1000	0.1000	0.0976	0.0973	0.0999	0.1001
2	0.3000	0.3000	0.3005	0.3004	0.3002	0.3002	0.3000	0.3000	0.5000	0.5000	0.3002	0.3006
3	0.5004	0.5004	0.5003	0.5002	0.5005	0.5005	0.4785	0.4785	0.6200	0.6032	0.5004	0.5005
4	0.7007	0.7007	0.7008	0.6993	0.7059	0.7004	0.7007	0.7007	0.9870	0.8765	0.7007	0.7007
5	1.0019	1.0008	1.0010	1.0010	0.9999	1.0004	1.0000	1.0000	1.0010	1.0010	1.0201	

Comparing the results of uniform cross sectional bars subjected to moving heat source, it is noticed that as the different vibrational modes increases, the real part of the nondimensional frequency $R(\xi)$ obtained for the polygonal cross sectional bar increases whereas the imaginary part $I(\xi)$ decreases, which is the proper physical behavior that the dissipation of energy due to moving heat sources.

modes of bar with respect to the heat source distance $z=1$ and $z=2$ than in the case of triangular cross sectional bar. The frequencies increase for higher modes of vibrations, and the cross over points in the trend line indicates the transfer of heat energy between the modes of vibrations.

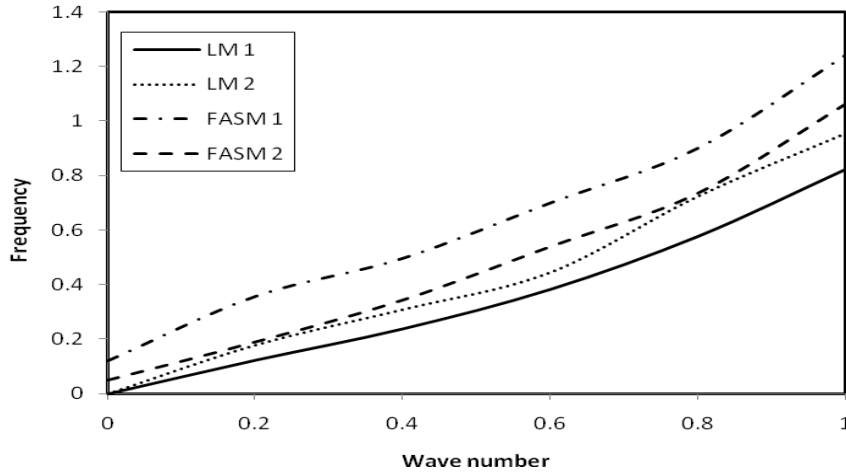


Fig. 4. Non dimensional frequency versus dimensionless wave number of a pentagonal bar for $z=1$ with $\alpha' = 2.0$, $\chi_1 = 2.6 \times 10^{-7}$, $\chi_2 = \chi_3 = 1.0$.

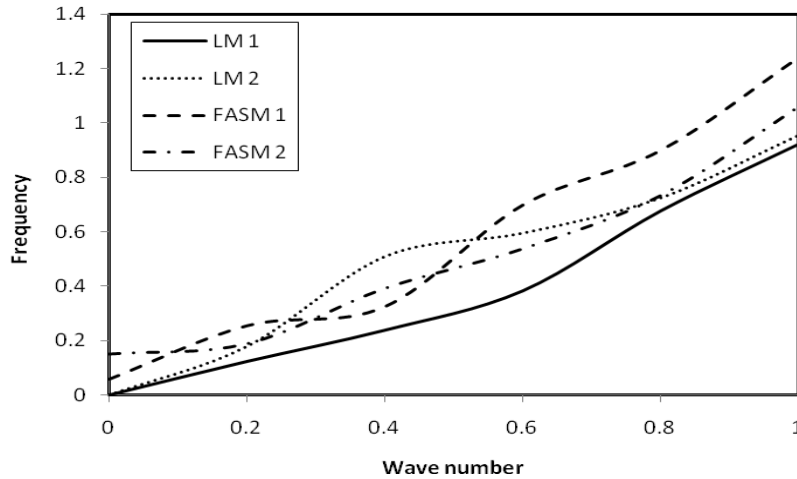


Fig. 5. Non dimensional frequency versus dimensionless wave number of a pentagonal bar for $z=2$ with $\alpha' = 2.0$, $\chi_1 = 2.6 \times 10^{-7}$, $\chi_2 = \chi_3 = 1.0$.

5.2. Square and Hexagonal cross-sections. In case of longitudinal vibration of square and hexagonal cross-sectional bars, the displacements are symmetrical about both major and minor axes, since both the cross-sections are symmetric about both the axes. Therefore the frequency equation is obtained by choosing both terms of n and m as $0, 2, 4, 6, \dots$ in Eq. (23). During flexural motion, the displacements are antisymmetrical about the major axis and symmetrical about the minor axis. Hence the frequency equation is obtained by choosing $n, m=1, 3, 5$ in Eq. (25).

A graph is drawn between the non-dimensional frequency Ω versus dimensionless wave number $|\zeta|$ of transversely isotropic square cross sectional bar for longitudinal and flexural (antisymmetric) modes of vibrations with the heat source distance $z=1$ and $z=2$ which is shown in Figs. 6 and 7. From Figures 6 and 7, it is clear that, the displacement of energy in the first mode and second mode of vibrations of longitudinal and flexural (antisymmetric)

developing of reliable finite elements and boundary elements for approximate solution of the problems of wave propagation in structures with moving heat sources.

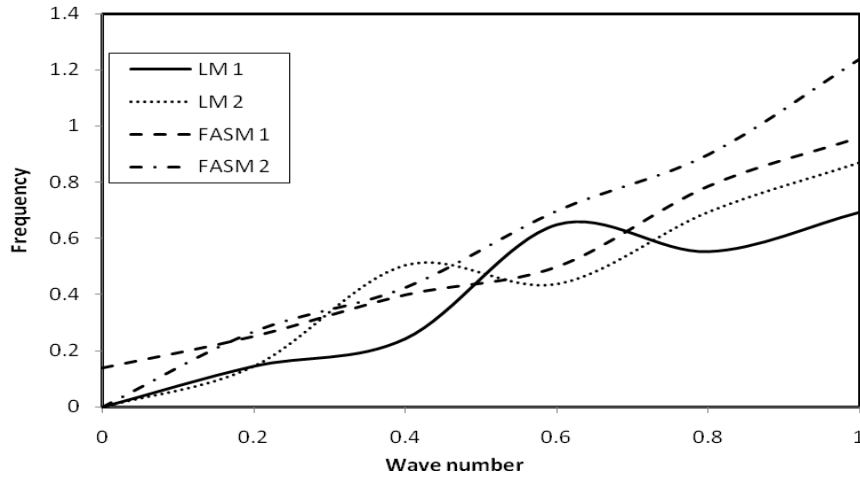


Fig. 8. Non dimensional frequency versus dimensionless wave number of a hexagonal bar for $z = 1$ with $\alpha' = 2.0$, $\chi_1 = 2.6 \times 10^{-7}$, $\chi_2 = \chi_3 = 1.0$.

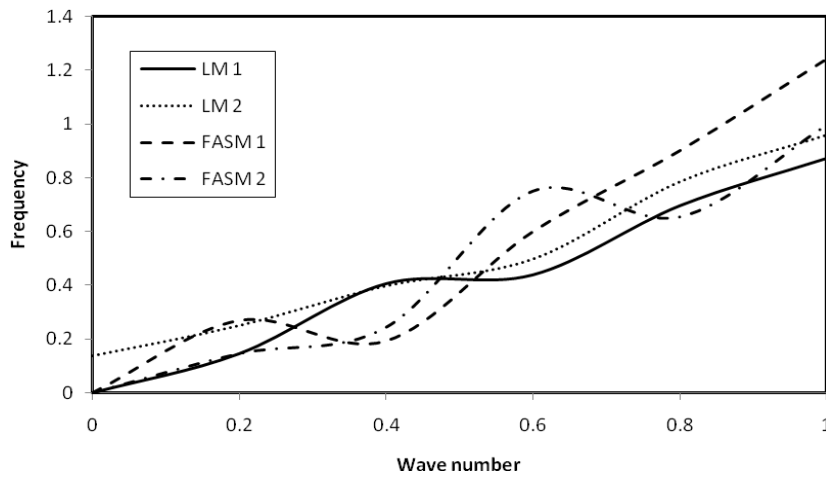


Fig. 9. Non dimensional frequency versus dimensionless wave number of a hexagonal bar for $z = 2$ with $\alpha' = 2.0$, $\chi_1 = 2.6 \times 10^{-7}$, $\chi_2 = \chi_3 = 1.0$.

6. Conclusions

In this paper, the dynamic response of a heat conducting solid bar of polygonal cross section subjected to moving heat source is analyzed by satisfying the boundary conditions on the irregular boundary using the Fourier expansion collocation method and the frequency equation for the longitudinal and flexural vibrations are obtained. Numerically the frequency equations are analyzed for the bar of different cross-section such as triangular, square, pentagonal and hexagonal. From the results of the present method, it is clear that moving heat source and the different geometrical cross sections of the bar influence the frequency. The problem can be analyzed for any other cross section by using the proper geometric relation.

Appendix A

The expressions $e_n^j \sim \bar{k}_n^j$ used in Eqs. (19) and (21) are given as follows:

$$e_n^j = 2\varepsilon_4 \left\{ n(n-1)J_n(\alpha_j ax) + (\alpha_j ax)J_{n+1}(\alpha_j ax) \right\} \cos 2(\theta - \gamma_l) \cos n\theta$$

$$\begin{aligned}
& -x^2 \left\{ \varepsilon_4 (\alpha_j a)^2 + \left[\bar{\lambda} + 2 \cos^2(\theta - \gamma_l) \right] + \bar{\lambda} d_j \varepsilon_4 \zeta \right\} J_n(\alpha_j ax) \cos n\theta \\
& + 2n\varepsilon_4 \left\{ (n-1)J_n(\alpha_j ax) - (\alpha_j ax)J_{n+1}(\alpha_j ax) \right\} \sin n\theta \sin 2(\theta - \gamma_l), \quad j=1,2,3 \quad (\text{A.1})
\end{aligned}$$

$$\begin{aligned}
e_n^4 &= 2\varepsilon_4 \left\{ n(n-1)J_n(\alpha_4 ax) - (\alpha_4 ax)J_{n+1}(\alpha_4 ax) \right\} \cos n\theta \cos 2(\theta - \gamma_l) \\
& + 2\varepsilon_4 \left\{ [n(n-1) - (\alpha_4 ax)^2]J_n(\alpha_4 ax) + (\alpha_4 ax)J_{n+1}(\alpha_4 ax) \right\} \sin n\theta \sin 2(\theta - \gamma_l), \quad (\text{A.2})
\end{aligned}$$

$$\begin{aligned}
f_n^j &= 2 \left\{ [n(n-1) - (\alpha_j ax)^2]J_n(\alpha_j ax) + (\alpha_j ax)J_{n+1}(\alpha_j ax) \right\} \cos n\theta \sin 2(\theta - \gamma_l) \\
& + 2n \left\{ (\alpha_j ax)J_{n+1}(\alpha_j ax) - (n-1)J_n(\alpha_j ax) \right\} \sin n\theta \cos 2(\theta - \gamma_l), \quad j=1,2,3 \quad (\text{A.3})
\end{aligned}$$

$$\begin{aligned}
f_n^4 &= 2n\varepsilon_4 \left\{ (n-1)J_n(\alpha_4 ax) - (\alpha_4 ax)J_{n+1}(\alpha_4 ax) \right\} \cos n\theta \sin 2(\theta - \gamma_l) \\
& - \varepsilon_4 \left\{ 2(\alpha_4 ax)J_{n+1}(\alpha_4 ax) - [(\alpha_4 ax)^2 - 2n(n-1)]J_n(\alpha_4 ax) \right\} \sin n\theta \cos 2(\theta - \gamma_l), \quad (\text{A.4})
\end{aligned}$$

$$g_n^j = (\zeta + d_j) \left\{ nJ_n(\alpha_j ax) \cos(\overline{n-1}\theta + \gamma_l) - (\alpha_j ax)J_{n+1}(\alpha_j ax) \cos(\theta - \gamma_l) \cos n\theta \right\}, \quad j=1,2,3 \quad (\text{A.5})$$

$$g_n^4 = \zeta \left\{ nJ_n(\alpha_4 ax) \cos(\overline{n-1}\theta + \gamma_l) - (\alpha_4 ax)J_{n+1}(\alpha_4 ax) \sin n\theta \sin(\theta - \gamma_l) \right\} \quad (\text{A.6})$$

$$k_n^j = e_j \left\{ n \cos(\overline{n-1}\theta + \gamma_l) J_n(\alpha_j ax) - (\alpha_j ax)J_{n+1}(\alpha_j ax) \cos(\theta - \gamma_l) \cos n\theta \right\}, \quad j=1,2,3 \quad (\text{A.7})$$

$$\begin{aligned}
\bar{e}_n^{-j} &= 2\varepsilon_4 \left\{ n(n-1)J_n(\alpha_j ax) + (\alpha_j ax)J_{n+1}(\alpha_j ax) \right\} \cos 2(\theta - \gamma_l) \sin n\theta \\
& - x^2 \left\{ \varepsilon_4 (\alpha_j a)^2 + \left[\bar{\lambda} + 2 \cos^2(\theta - \gamma_l) \right] + \bar{\lambda} d_j \varepsilon_4 \zeta \right\} J_n(\alpha_j ax) \cos n\theta \\
& - 2n\varepsilon_4 \left\{ (n-1)J_n(\alpha_j ax) - (\alpha_j ax)J_{n+1}(\alpha_j ax) \right\} \cos n\theta \sin 2(\theta - \gamma_l), \quad j=1,2,3 \quad (\text{A.8})
\end{aligned}$$

$$\begin{aligned}
\bar{e}_n^{-4} &= 2\varepsilon_4 \left\{ n(n-1)J_n(\alpha_4 ax) - (\alpha_4 ax)J_{n+1}(\alpha_4 ax) \right\} \sin n\theta \cos 2(\theta - \gamma_l) \\
& - 2\varepsilon_4 \left\{ [n(n-1) - (\alpha_4 ax)^2]J_n(\alpha_4 ax) + (\alpha_4 ax)J_{n+1}(\alpha_4 ax) \right\} \cos n\theta \sin 2(\theta - \gamma_l), \quad (\text{A.9})
\end{aligned}$$

$$\begin{aligned}
\bar{f}_n^j &= 2 \left\{ [n(n-1) - (\alpha_j ax)^2]J_n(\alpha_j ax) + (\alpha_j ax)J_{n+1}(\alpha_j ax) \right\} \sin n\theta \sin 2(\theta - \gamma_l) \\
& - 2n \left\{ (\alpha_j ax)J_{n+1}(\alpha_j ax) - (n-1)J_n(\alpha_j ax) \right\} \cos n\theta \cos 2(\theta - \gamma_l), \quad j=1,2,3 \quad (\text{A.10})
\end{aligned}$$

$$\begin{aligned}
\bar{f}_n^4 &= 2n\varepsilon_4 \left\{ (n-1)J_n(\alpha_4 ax) - (\alpha_4 ax)J_{n+1}(\alpha_4 ax) \right\} \sin n\theta \sin 2(\theta - \gamma_l) \\
& + \varepsilon_4 \left\{ 2(\alpha_4 ax)J_{n+1}(\alpha_4 ax) - [(\alpha_4 ax)^2 - 2n(n-1)]J_n(\alpha_4 ax) \right\} \cos n\theta \cos 2(\theta - \gamma_l), \quad (\text{A.11})
\end{aligned}$$

$$\bar{g}_n^{-j} = (\zeta + d_j) \left\{ nJ_n(\alpha_j ax) \cos(\overline{n-1}\theta + \gamma_l) - (\alpha_j ax)J_{n+1}(\alpha_j ax) \cos(\theta - \gamma_l) \sin n\theta \right\}, \quad j=1,2,3 \quad (\text{A.12})$$

$$\bar{g}_n^{-4} = \zeta \left\{ nJ_n(\alpha_4 ax) \cos(\overline{n-1}\theta + \gamma_l) + (\alpha_4 ax)J_{n+1}(\alpha_4 ax) \cos n\theta \sin(\theta - \gamma_l) \right\} \quad (\text{A.13})$$

$$\bar{k}_n^{-j} = e_j \left\{ n \cos(\overline{n-1}\theta + \gamma_l) J_n(\alpha_j ax) + (\alpha_j ax)J_{n+1}(\alpha_j ax) \cos(\theta - \gamma_l) \sin n\theta \right\}, \quad j=1,2,3 \quad (\text{A.14})$$

References

- [1] D.C. Gazis // *Journal of Acoustical Society of America* **31** (1964) 568.
- [2] I. Mirsky // *Journal of Acoustical Society of America* **36** (1964) 41.
- [3] K. Nagaya // *Journal of Acoustical Society of America* **49** (1982) 157.
- [4] K. Nagaya // *Journal of Vibration and Acoustics* **105** (1983) 132.
- [5] K. Nagaya // *Journal of Acoustical Society of America* **75(3)** (1984) 834.
- [6] K. Nagaya // *Journal of Acoustical Society of America* **77(5)** (1985) 1824.
- [7] H.S. Paul // *Journal of Acoustical Society of America* **82(6)** (1987) 2013.
- [8] F. Ashida // *Archive of applied Mechanics* **71** (2003) 221.
- [9] F. Ashida // *Acta Mechanica* **161** (2003) 1.
- [10] T.R. Tauchert, F. Ashida, N. Noda, S. Adali, V. Verijenko // *Composite structures* **48** (2000) 31.
- [11] C.F. Gao, N. Noda // *International Journal of Engineering Sciences* **42**(2004) 1347.
- [12] W.Q. Chen, C.W. Lim, H.J. Ding // *Engineering Analysis with Boundary Elements* **29** (2005) 524.
- [13] E.S. Suhubi // *Journal Mechanics Physics and Solids* **12** (1964) 69.
- [14] E.S. Erbay, E.S. Suhubi // *Journal of Thermal Stresses* **9** (1986) 279.
- [15] H.W. Lord, Y. Shulman // *Journal of Mechanics Physics and Solids* **5**(1967) 299.
- [16] A.E. Green, K.A. Lindsay // *Journal of Elasticity* **2** (1972) 1.
- [17] A.E. Green, N. Laws // *Archive of Rational Mechanical Analysis* **45** (1972) 47.
- [18] C.B. Hallam, E. Ollerton // *Journal of Strain Analysis* **8(3)** (1973) 160.
- [19] H. Singh, J.N. Sharma // *Journal of Acoustical Society of America* **77(3)** (1985) 1046.
- [20] J.N. Sharma, R.S. Sidhu // *International Journal of Engineering Science* **24(9)** (1986) 1511.
- [21] K.L. Verma // *International Journal of Engineering Science* **40** (2002) 2077.
- [22] J.N. Sharma // *Journal of Acoustical Society of America* **110(1)** (2001) 254.
- [23] M. Savoia, J.N. Reddy // *Journal of Mechanics Physics and Solids* **32(5)** (1995) 593.
- [24] R. Selvamani // *Materials Physics and Mechanics* **19** (2014) 51.
- [25] P. Ponnusamy, R. Selvamani // *European Journal of Mechanics A/ Solids* **39** (2013) 76.
- [26] P. Ponnusamy, R. Selvamani // *Journal of Thermal Stresses* **35(12)** (2012) 1119.
- [27] N.S. Al-Huniti, M.A. Al-Nimr, M. Naji // *Journal of Sound and Vibration* **242(4)** (2001) 629.
- [28] A. Baksi, R.K. Bera, L. Debnath // *International Journal of Engineering Science* **43** (2005) 1419.
- [29] G. Lykotrafitis, H.G. Georgiadis // *International Journal of Solids and Structures* **40** (2003) 899.
- [30] C.K. Hsieh // *ASME Journal of Heat Transfer* **117** (1995) 1076.
- [31] E.S. Suhubi, In: *Continuum Physics (Academic, New York, 1975)*, Vol. II, Chapter 2.
- [32] H.M. Antia // *Hindustan Book Agency, New Delhi* (2002).